AGU100 ADVANCING EARTH AND SPACE SCIENCE

Geophysical Research Letters

RESEARCH LETTER
10.1029/2018GL079033

Contributions of Internal Variability and External Forcing to the Recent Pacific Decadal Variations

Wenjian Hua[1,2], Aiguo Dai[2], and Minhua Qin[1,2]

[1]Key Laboratory of Meteorological Disaster, Ministry of Education (KLME)/Joint International Research Laboratory of Climate and Environment Change (ILCEC)/Collaborative Innovation Center on Forecast and Evaluation of Meteorological Disasters (CIC-FEMD), Nanjing University of Information Science and Technology, Nanjing, China, [2]Department of Atmospheric and Environmental Sciences, University at Albany, State University of New York, Albany, NY, USA

Key Points:

- Observed Pacific decadal variations were dominated by internal variability during 1920–2016
- However, greenhouse gases and other external forcings have had a large contribution to Pacific SST variations since the 1990s
- Anthropogenic aerosols induced multiyear to decadal SST variations in the Pacific and contributed to a La Niña-like pattern since 1998

Supporting Information:

- Supporting Information S1

Correspondence to:
A. Dai,
adai@albany.edu

Citation:
Hua, W., Dai, A., & Qin, M. (2018). Contributions of internal variability and external forcing to the recent Pacific decadal variations. *Geophysical Research Letters*, *45*, 7084–7092. https://doi.org/10.1029/2018GL079033

Received 30 MAR 2018
Accepted 26 JUN 2018
Accepted article online 3 JUL 2018
Published online 16 JUL 2018

The copyright line for this article was changed on 19 JUN 2019 after original online publication.

Abstract There is substantial uncertainty in the relative contributions of internal variability and external forcing to the recent Pacific decadal variability, especially regarding their linkage with the Interdecadal Pacific Oscillation. By analyzing observations and large ensembles of coupled climate model simulations, here we show that observed Pacific decadal variations since 1920 resulted primarily from internal variability, although greenhouse gas (GHG) and other external forcing did modulate decadal variations in Pacific sea surface temperatures (SSTs) significantly, especially for the period since the early 1990s. Specifically, the GHG-induced warming and the recovery from the volcanic cooling caused by the 1991 Pinatubo eruption led to large warming in the tropical Pacific during 1993–2012, while recent anthropogenic aerosols contributed to Pacific regional SST variations on multiyear to decadal scales, causing a La Niña-like cooling pattern in the Pacific since 1998 in some of the models. Our results provide new evidence that both internal variability and external forcing have contributed to the recent decadal variations in Pacific SSTs since the early 1990s, although large uncertainties exist among the model-simulated effects of anthropogenic aerosols.

Plain Language Summary The Interdecadal Pacific Oscillation (IPO), the dominant mode of decadal to multidecadal variations of sea surface temperatures (SSTs) in the whole Pacific basin, has major impacts on global and regional climate. Given the large anthropogenic climate change during recent decades, it is natural to ask the following question: Are the recent IPO cycles also linked to anthropogenic forcing? Here we examine and attribute the roles of internal variability and external forcing in the recent IPO cycles through analyses of large ensembles of simulations by coupled climate models. Results suggest that while internal variability played a dominant role for the IPO cycles since 1920, the external forcing from volcanic and anthropogenic aerosols also contributed to the recent decadal variations in Pacific SSTs since the early 1990s. Our study contributes to the ongoing debate on the role of external forcing in recent decadal climate variability and improves current understanding of Pacific decadal variations, especially the relative role of external forcing and internal variability.

1. Introduction

The Interdecadal Pacific Oscillation (IPO; Power et al., 1999), or its North Pacific counterpart—the Pacific Decadal Oscillation (Mantua et al., 1997), is the leading mode of sea surface temperature (SST) variability on decadal to multidecadal time scales in the Pacific basin that broadly resembles El Niño-Southern Oscillation (ENSO)-related SST anomaly patterns (Zhang et al., 1997). The IPO impacts surface temperature and precipitation over many parts of the world (e.g., Dai, 2013; Dong & Dai, 2015; Gu & Adler, 2015) and causes decadal changes in global warming rates (Fyfe et al., 2016). In particular, the cooling in the eastern Pacific since around 1993 associated with the IPO phase changes is likely a major cause for the recent slow-down in the global surface warming rate since the late 1990s (Dai et al., 2015; Kosaka & Xie, 2013). Given that the recent Pacific climate may be linked to natural and anthropogenic external forcings (Smith et al., 2016), it is natural to ask whether the recent IPO cycles and the many associated changes are linked to any of the external forcings, including the decadal changes in anthropogenic and natural aerosols (Meehl et al., 2013).

The Pacific Ocean has experienced remarkable changes since the early 1990s, including the strengthening of Pacific trade winds, the Walker circulation, and oceanic heat uptake (England et al., 2014). The accelerated Pacific trade winds and wind-driven ocean circulation are partly attributed to external

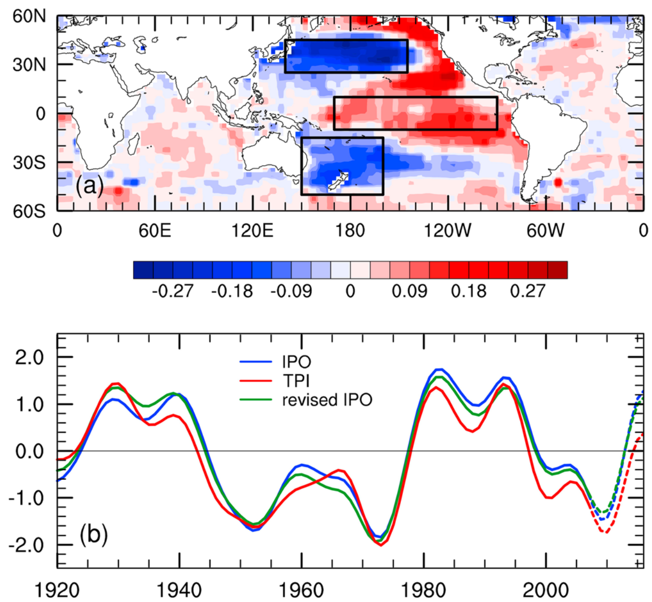

Figure 1. (a) The pattern of the Interdecadal Pacific Oscillation (IPO) obtained by regressing 13-year low-pass filtered sea surface temperature (SST) anomalies from 1920 to 2016 from observational data set HadCRUT4 onto the revised IPO index (green line in (b)). The spatial patterns are similar when the IPO or TPI index is used in the regression. (b) The standardized time series of three IPO indices based on HadCRUT4 data (unit: standard deviation). The IPO index (blue line) is defined as the second empirical orthogonal function (EOF) mode of 13-year smoothed SST anomaly fields over the Pacific Ocean (40°S–60°N, 105°E–70°W). The Tripole Index (TPI, red line) is defined as the difference of the SST anomalies between the central equatorial Pacific (TP: 10°S–10°N, 170°E–90°W) and the mean of the northwestern (NP: 25°–45°N, 140°E–145°W) and southwestern (SP: 50°–15°S, 150°E–160°W) Pacific regions outlined in (a). The revised IPO index (green line) is defined as the first EOF of 13-year low-pass filtered Pacific SSTs from HadCRUT4 after the component correlated with the multimodel ensemble mean of the 122 all-forcing simulations by 39 CMIP5 models was removed at each grid point prior to the EOF analysis. The last 9 years, plotted using dashed lines in (b), used mirrored data in the filtering and thus are less reliable.

forcing (Allen et al., 2014), with about one third of the trade wind intensification being attributed to sulfate aerosols since the 1990s (Takahashi & Watanabe, 2016). Aerosols emitted from North America and East Asia can influence the Aleutian low and Pacific trade winds, thereby affecting Pacific SSTs (Boo et al., 2015). The warming in the Indian and Atlantic Ocean may also have contributed to the recent strengthening of Pacific trade winds and Walker circulation and thus the La Niña-like pattern (Luo et al., 2012; McGregor et al., 2014). Since the Indian Ocean warming likely has resulted from increases in greenhouse gases (GHGs; Myhre et al., 2013) and aerosol forcing may have played a significant role for the recent SST changes in the Atlantic Ocean (Booth et al., 2012), the exact roles of internal variability (IV) and external forcing in recent Pacific decadal variations, especially their linkage with the recent IPO phase changes, are still not well understood.

This study aims to examine and attribute the roles of IV and external forcing in the recent IPO cycles through analyses of a large ensemble of simulations by the Coupled Model Intercomparison Project Phase 5 (CMIP5) models. We first revisit the characteristics of the IPO mode using different approaches and then quantify the externally forced and internally generated Pacific decadal variations during recent decades. Our results should improve current understanding of Pacific decadal variations, especially its response to external forcing and the role of IV.

2. Data, Model Simulations, and Methods

2.1. Observational Data and Model Simulations

We used the HadCRUT4 global gridded monthly surface temperature data, which combine the CRUTEM4 land surface air temperature and the HadSST3 SST (Morice et al., 2012). We focus on the period from 1920 to 2016, as SST data over the tropical Pacific are sparse before around 1920 (Deser et al., 2010). We also used other SST data sets to examine the Pacific decadal variations, for example, the Kaplan Extended SST (Kaplan et al., 1998), COBE SST (Hirahara et al., 2014), and ERSSTv5 (Huang et al., 2017). The results are qualitatively similar and thus not included in the figures shown here.

The first set of model simulations were from the CMIP5 (Taylor et al., 2012). Monthly surface temperature data were obtained from the all-forcing historical (1920 to 2005) and RCP4.5 (2006 to 2100) simulations from 39 models (Table S1 in the supporting information). The effects of different external forcing agents (Table S2) were investigated by considering simulations (only up to 2012) forced separately by GHGs, anthropogenic forcing, anthropogenic aerosols, volcanic aerosols, and natural (volcanic aerosols plus solar) forcing. Note that CMIP5 models did not include the effects of a series of small volcanic eruptions after 2005, which may contribute to the warm bias in these model simulations (Santer et al., 2014).

2.2. Methods

Many different methods have been used to define the index and spatial patterns associated with the IPO. A common method is to use a leading empirical orthogonal function (EOF) of the global or Pacific SST fields to define the IPO (Dai, 2013; Meehl et al., 2009). Here we first define the conventional IPO index as the second EOF mode of low-passed SST anomaly fields in the Pacific Ocean (40°S–60°N, 105°E–70°W) during 1920–2016, as the first EOF primarily represents the forced global warming mode. Interannual to multiyear variations were removed at each grid point using low-pass filtering (using a 19-point Lanczos filter with a 13-year cutoff period) prior to the EOF analysis. We also used the Tripole Index (TPI; Henley et al., 2015), which is calculated as the SST anomaly difference between the central equatorial Pacific (TP: 10°S–10°N, 170°E–90°W) and the mean averaged over the northwestern (NP: 25°–45°N, 140°E–145°W) and southwestern (SP: 50°–15°S,

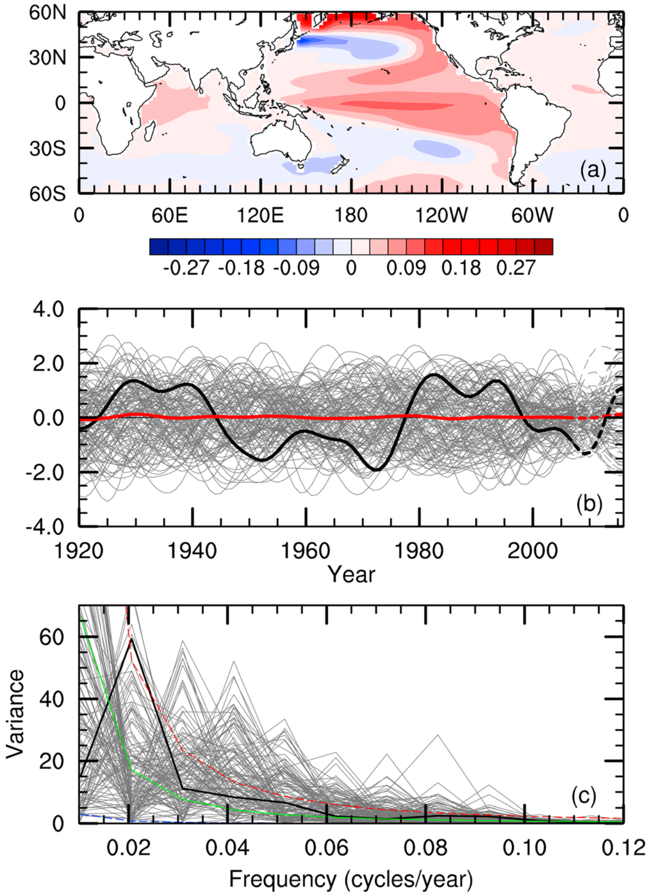

Figure 2. (a) The ensemble average of the first empirical orthogonal function pattern of the sea surface temperature (SST) fields from each of the 122 all-forcing historical (for 1920–2005) and RCP4.5 (for 2006–2016) simulations by 39 CMIP5 models after removing the multimodel ensemble mean locally from the SST data series. (b) The revised Interdecadal Pacific Oscillation (IPO) index from individual model runs (grey), and their ensemble mean (red), compared with that from observations (black). The last 9 years, plotted using dashed lines in (b), used mirrored data in the filtering and thus are less reliable. (c) The power spectrum of the IPO indices from observations (black line in (b)) and individual model simulations (gray lines in (b)). The green, blue, and red curves in (c) show the red noise confidence curve and 5% and 95% confidence bounds, respectively.

150°E–160°W) Pacific regions. To extend the time series as close to the present as possible, mirrored end points were used in the low-pass filtering. This approach seems to work reasonably well when comparing with the unfiltered series, although clearly the smoothed indices near the two ends need to be used with caution. Further, the smoothed indices shift to a positive phase around 2014 due to the unusually warm 2014–2016 El Niño event.

To reduce the chance of aliasing between the internal IPO-induced and externally forced changes in SSTs, following Dai et al. (2015) and Steinman et al. (2015), we used the CMIP5 multimodel ensemble mean (MME, with 122 runs from 39 models) at each grid point as the first-order estimate of the local forced signal and removed it through regression from the SST time series from observations or individual model runs to produce the residual SST fields that contain primarily internal climate variations (Dai & Bloecker, 2018; Xu & Hu, 2018). After the forced signal is removed, we define the first EOF of the low-pass filtered Pacific SSTs as the revised IPO mode. This revised procedure accounts for both the spatial heterogeneity and temporal nonlinearity in the externally forced long-term warming trend and removes it from other variations in the data series. Since many of the CMIP5 models did not include aerosols' indirect effects that account for the majority of the aerosols' total effect over oceans (Allen et al., 2015; Williams et al., 2001; Zhang et al., 2013), we repeated our analyses using only those CMIP5 models that included both the direct and indirect effect and found that the results are similar (see Figures S3 and S4). This suggests that aerosols (when both effects are accounted for) play only a modest role in driving Pacific decadal variability through the full historical period, in contrast to the Atlantic basin (Bellucci et al., 2017; Booth et al., 2012).

3. Results

3.1. The Characteristics of the IPO Mode in Observations and Climate Models

The IPO-associated SST patterns (Figure 1a) show opposite anomalies between the central-eastern tropical Pacific and the western-central North and South Pacific, with broader and weaker SST anomalies in the equatorial tropics than those for ENSO but stronger anomalies in the central North Pacific, consistent with Dong et al. (2018). To capture the Pacific-wide interdecadal variability, we examined and compared three IPO indices (Figure 1b), which are highly correlated ($r > 0.95$) and all exhibit similar remarkable decadal to multidecadal variations. They show a cold or negative phase from the early 1940s to late 1970s and from around 1999 to present and a warm or positive phase from the 1920s to early 1940s and from late 1970s to the late 1990s. The exact years for the phase change may vary slightly, depending on how the index series is smoothed and what time period (which affects the zero line) is analyzed. The similarity between the revised IPO index, which explicitly excluded the externally forced signal in the SST fields, and the other two indices, which could potentially still contain some of the forced signal as their construction methods do not guarantee the removal of all the forced signal, suggest that the IPO cycles from all three methods are primarily internally generated variations; that is, the other two methods effectively remove most of the externally forced signal from the IPO indices. Since the revised IPO index was derived by explicitly removing the externally forced nonlinear signal, we will use this index in the following analyses, and it is simply referred to as the IPO index.

Figure 2b shows the model-simulated IPO index from individual historical all-forcing simulations. Although the multimodel ensemble-mean IPO patterns are similar to those from the observations (Figure 2a), the

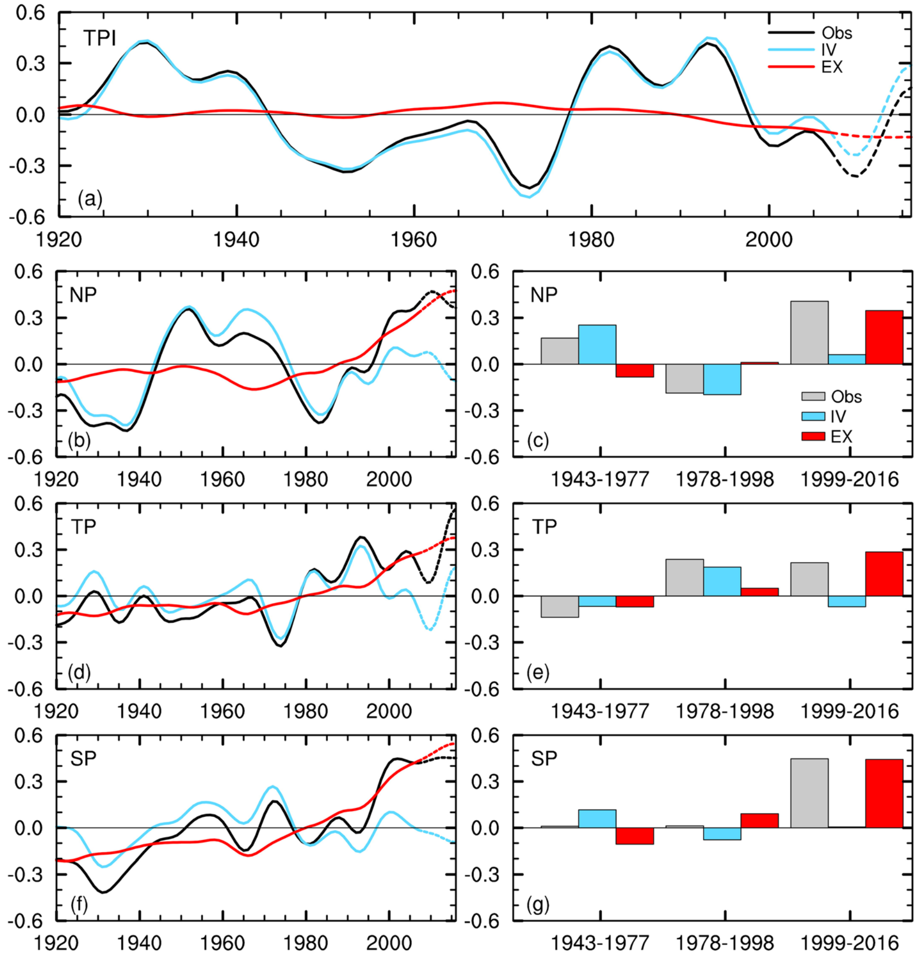

Figure 3. (a) Time series of the sea surface temperature (SST) difference (°C) between TP (central equatorial Pacific, 10°S–10°N, 170°E–90°W) and the mean of NP (northwestern Pacific, 25°–45°N, 140°E–145°W) and SP (southwestern Pacific, 50°–15°S, 150°E–160°W; i.e., the Tripole Index (TPI) Interdecadal Pacific Oscillation (IPO) index, see Figure 1a) for the observations (Obs, black), estimated internal variability in the observations (IV, blue), and the externally forced signal based on CMIP5 model simulations (EX, red). Left column: Anomaly time series of regional mean SST (°C) from Obs, IV, and EX over the (b) NP, (d) TP, and (f) SP. Right column: The epoch-mean of the SST anomalies (°C) during three IPO phase periods for (c) NP, (e) TP, and (g) SP. We rescaled the multimodel ensemble mean of the surface temperature time series from the all-forcing historical simulations to the observed long-term change at each grid point via linear regression as the externally forced signal, and the difference between the observations and the external signal is used as the IV component in the observations.

temporal evolution is quite different among the individual simulations and from the observations. This is expected since the temporal evolution of the internally generated IPO is realization-dependent, so that it does not repeat itself among two different realizations (i.e., two different simulations).

The IPO in these 122 ensemble members varies randomly in phase, leading to a very small variance in the ensemble average of the IPO index from the individual runs (red line in Figure 2b), which are consistent with the results based on the 40-member Community Earth System Model large ensemble simulations (Si & Hu, 2017). The correlations of the IPO indices from observations and the model simulations have a mean around zero, with only 6% of the simulations being positively correlated significantly ($p < 0.1$) with the observed IPO index. This supports the notion that the IPO indices during 1920–2016 from both observations and the model simulations are mainly internally generated cycles that are realization-dependent. Power spectral analyses indicate that the observed IPO peaks around ~50 years (Figure 2c). The simulated IPO has multiple spectral peaks, such as at 13–20 and 25–50 years, in line with the results from the pre-industrial control run (Figure S2). Given the relatively short length of observational record, over which the models show varying spectral peaks, it is difficult to identify whether there is a robust spectral peak in the observations.

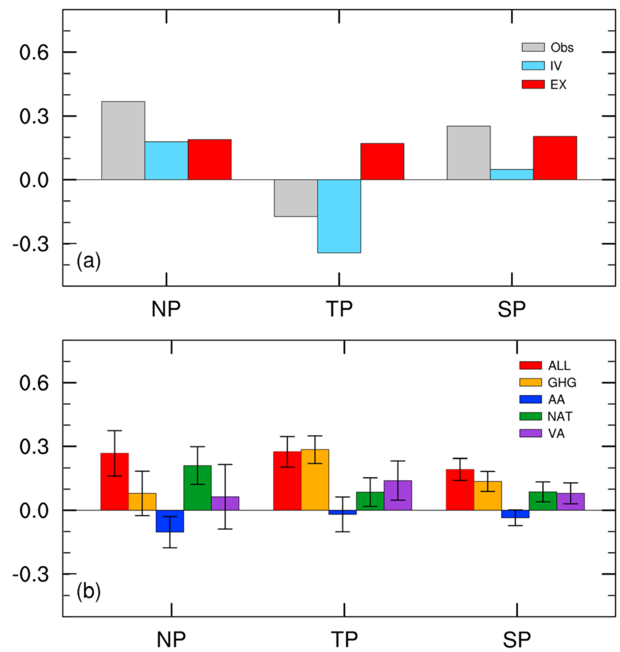

Figure 4. (a) Regional sea surface temperature linear trends for the three outlined boxes in Figure 1a for the period from 1993 to 2012 (°C per decade) from observations (Obs, gray), internal variability (IV, blue), and external forcing (EX, red). (b) Same as (a) but from the CMIP5 multimodel ensemble mean of All and single forcing (i.e., greenhouse gas [GHG], anthropogenic aerosols [AA], natural forcing [NAT], and volcanic aerosols [VA]) simulations. The error bars denote the standard deviation of intermodel variations. The CMIP5 single forcing multimodel ensemble mean was defined as the arithmetic mean of the ensemble mean for each model, with the same weight for each model, as different models had different numbers of realizations. NP = northwestern Pacific, TP = central equatorial Pacific, SP = southwestern Pacific.

3.2. Forced Versus Internal Pacific Decadal Variations

Unlike the internally generated IPO mode discussed above, Pacific decadal to multidecadal variations in SST and other fields are also modulated by external anthropogenic and natural forcing (Dong et al., 2014; Meehl et al., 2009). In this section, we further examine the potential influences of the external forcing on the Pacific regional decadal variability.

To capture the Pacific climate variations at the regional scales, we focus on the TPI regions (i.e., NP, TP, and SP; Figure 1a). The SST series contain both forced changes and internal variations, and thus, they can help quantify the relative contributions of the externally forced and internally generated variations that are associated with the IPO mode. Using the SST difference between TP and the mean of NP and SP as the IPO index yields similar results for the two cases with the original observed SSTs and the estimated IV in the observations (Figure 3a), as the forced component is largely canceled out in the differencing. The externally forced (EX) component is much larger since the early 1990s, indicating an important role in influencing the Pacific regional SST variations (Figure 3a). This is discussed further in section 3.3.

Figures 3c, 3e, and 3g show the epoch-mean of the SST anomalies during the IPO phase periods. The three regional SST anomaly series all exhibit large decadal variations superimposed on an externally forced warming trend since 1920. The warming trend significantly raises the SST since the 1990s compared with the IV case for all the regions (Figures 3b, 3d, and 3f). Despite the overall warming trend in the observed SST series, strong correlations (r = 0.65–0.90, $p < 0.05$) exist between the observed and IV-induced SST series, and the epoch-mean anomalies are dominated by the IV component for all but the most recent period from 1999 to 2016. This further suggests a dominant role of IV in the observed Pacific decadal variations and the associated IPO phase transitions during 1920–2016, although the warming trend had a large contribution to the SST anomalies since the late 1990s.

3.3. Understanding the 1990s Shift

Figure 4a shows the SST trends during 1993–2012 from observations, the externally forced component, and the IV for the three TPI regions. The 1993–2012 period is chosen because the year 1993 is the time when the observed IPO indices peak and then start a declining trend, and the CMIP5 single forcing simulations end in 2012 (Figure 1b). As expected, these three regions exhibit the tripole pattern in the observed and IV-induced SST trends, with the TP being opposite to the other two regions. The observed SST trends are qualitatively consistent with the internally generated (i.e., IPO-induced) SST trends since 1993. The observed SST trend exhibits a cooling (warming) pattern in the central-eastern (western) Pacific that resembles the negative phase of the internally generated IPO pattern (Figures 5a and 5b).

We further examine CMIP5 single-forcing simulations. The model-simulated response to all external forcing leads to warming trends during 1993–2012 everywhere including the Pacific Ocean (Figure 5c), with most of the warming coming from the GHG forcing that induces an El Niño-like pattern (Figure 5e). Such a response pattern is consistent with the increased frequency of extreme El Niño events under GHG-induced global warming reported previously (Cai et al., 2015; Collins et al., 2010). The increased El Niño-like responses result from an enhanced probability of the establishment of atmospheric deep convection in the eastern equatorial Pacific, as the GHG-induced warming occurs faster than in the surrounding ocean waters (Cai et al., 2014).

The natural (NAT, Figure 5f) and volcanic (VA, Figure 5g) forcing simulations show a warming trend from 1993 to 2012 over most of the globe, with a weak ENSO-like pattern in the Pacific, as the system recovers from the

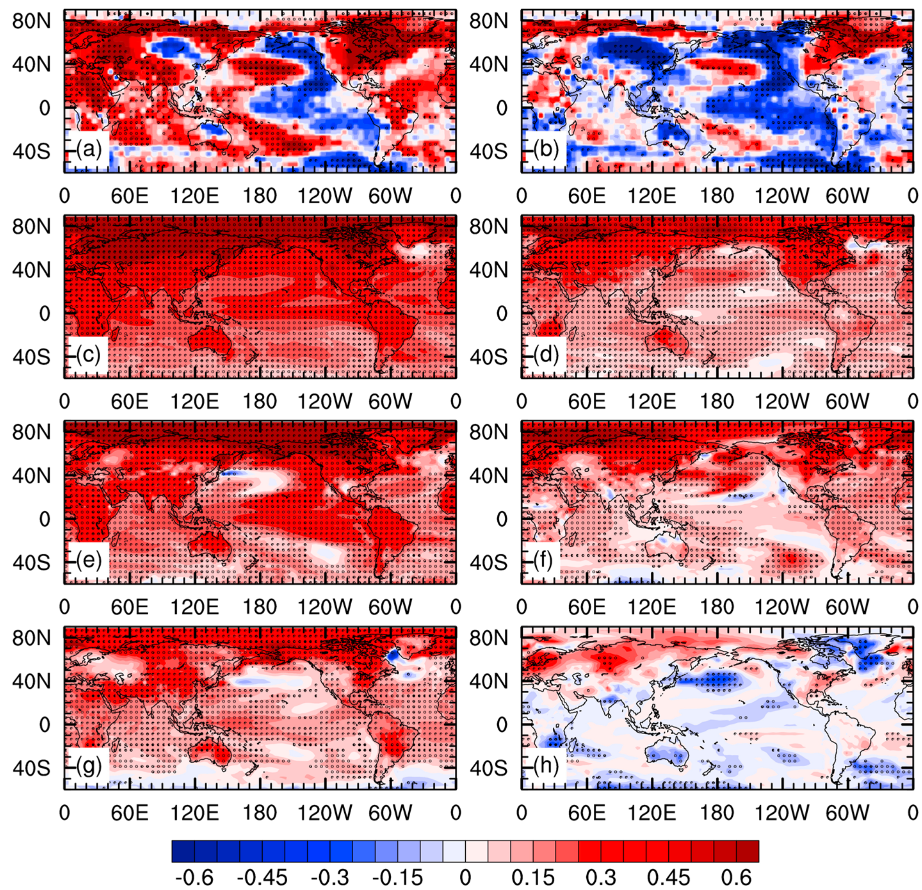

Figure 5. Spatial patterns of the surface temperature linear trend (°C per decade) for the period from 1993 to 2012 from (a) observations, (b) internal component in observations, and CMIP5 multimodel ensemble mean of simulations under (c) ALL, (d) anthropogenic forcing, (e) greenhouse gas, (f) natural forcing, (g) volcanic aerosols, and (h) anthropogenic aerosols forcing. The stippling indicates that the trend is statistically significant at the 5% level based on a two-sided Student *t* test.

cooling caused by the 1991 Pinatubo volcanic eruption (e.g., Adams et al., 2003; Li et al., 2013; Maher et al., 2015; Mann et al., 2005). The CMIP5 models with volcanic forcing (Figures S5 and S6) confirm that the volcanic forcing causes a La Niña-like response (i.e., more cooling in the central and eastern tropical Pacific than in the western Pacific) during the few years after the eruption; thereafter, the system recovers from this cooling pattern, leading to a warming trend pattern in the tropical Pacific (Figures 5f and 5g). Recently, Khodri et al. (2017) suggested that the volcanic cooling over tropical Africa alters tropical Kelvin waves that may lead to an El Niño-like response to the volcanic forcing over the Pacific, which is not evident in Figure S5. How the tropical atmosphere-ocean system responds to the radiative forcing of volcanic eruptions needs further investigation.

The model-simulated response to anthropogenic aerosols during 1993–2012 varies greatly among individual models (Figures 4b and S7), with large cooling trends in the North Pacific around 40°N but weak positive SST trends in the eastern tropical Pacific (Figure 5h). For the longer period from 1920 to 2012, the SST anomalies exhibit large decadal variations superimposed on an aerosol-forced cooling trend since 1920 (Figure S8). Multimodel ensemble mean results show that anthropogenic aerosols caused some cooling in the North Pacific in the 1970s and 1980s; thereafter, the cooling effect is small (Figure S8b). The effects on the tropical and South Pacific regions are small (Figures S8d and S8f). Interestingly, anthropogenic aerosols caused a trend pattern since 1998 that resembles the negative phase of the IPO/Pacific Decadal Oscillation in the CanESM2, CCSM4, GFDL-CM3, and GISS-E2-H models (all with an ensemble size greater than 3) and multimodel ensemble mean from all 11 models (Figure S9). Smith et al. (2016) suggested that anthropogenic aerosol emissions from the United States and China have influenced the Pacific Decadal Oscillation through their impacts on the Aleutian Low during the recent warming hiatus period since ~1999. Our results show that the North Pacific SST changes in response to anthropogenic aerosols exhibit multiyear to decadal variations between the 1990s and 2000s that differ considerably among the models, and the Pacific decadal shift in the 1990s is caused by both internal climate variability and aerosol changes, consistent with Smith et al. (2016).

4. Conclusions and Discussion

In this study, we have analyzed observational data and large ensembles of coupled model simulations to examine and attribute the roles of IV and external forcing in the recent IPO cycles. We first investigated and compared the IPO mode since 1920 defined using different methods. The results suggest that the three detrending approaches all effectively remove the externally forced signal from the IPO indices, as the IPO mode reflects primarily internally generated variations. The IPO-associated SST pattern is well simulated in both pre-industrial control runs and all-forcing historical simulations by many models, but the IPO phase is realization-dependent as expected.

Analyses of the SST changes in the three TPI regions further confirm the dominant role of IV in influencing the Pacific decadal variations and the associated IPO phase transitions during 1920–2016, although the externally forced warming trend had a large contribution to the observed SST anomalies since the 1990s. The observed SST trends during 1993–2012 are qualitatively consistent with the internally generated (i.e., IPO-induced) SST changes, while the externally forced component leads to warming trends throughout the Pacific Ocean. Recent GHG forcing leads to faster surface warming in the eastern than in the western equatorial Pacific and induces an El Niño-like warming pattern. Both the mean state and the ENSO activities in the tropical Pacific are expected to change under GHG-induced global warming, with more eastward-propagating El Niño events and more extreme ENSO events (Cai et al., 2014; Collins et al., 2010). The recovering from the cooling caused by the 1991 Pinatubo volcanic eruption led to warming trends in the tropical Pacific and other regions during 1993–2012. This causes decadal changes in the tropical Pacific that resemble an ENSO-like warming pattern in the postvolcanic years.

The SST response to anthropogenic aerosols exhibits large multiyear to decadal variations in the three TPI regions that differ considerably among the models. Some models (e.g., CanESM2, CCSM4, GFDL-CM3, and GISS-E2-H, with ensemble size greater than 3) show a La Niña-like cooling response to anthropogenic aerosols in the Pacific since the year 1998, but this is absent in other models. Given that the majority of current climate models poorly represent the aerosol-cloud interactions, especially aerosols' indirect effects on cloud albedo and lifetime (Boucher et al., 2013), such a diverse response is not unexpected.

Our results highlight that while greenhouse forcing dominated the regional SST warming trends from 1920 to 2016, the external forcing from volcanic and anthropogenic aerosols significantly contributed to the different Pacific regional SST variations since the early 1990s. However, current climate models have substantial biases in simulating the SST variations since the 1980s (Fyfe & Gillett, 2014). The biases may result from errors in simulating the external forcing and model response or due to different realizations of internal climate variability in models (Fyfe et al., 2013). Luo et al. (2018) found that the current CMIP5 models underestimate interbasin warming contrast in the tropics and the local SST-cloud negative feedback in the equatorial Pacific. Further efforts to explore the interbasin interactions and to reduce the model biases could help improve simulations of the externally forced climate variations and advance our understanding of decadal variability in the Pacific.

Acknowledgments
This study was partly funded by the National Key R&D Program of China (2017YFC1502101). A. Dai was supported by the US National Science Foundation (grant AGS-1353740 and OISE-1743738), the US Department of Energy's Office of Science (award DE-SC0012602), and the US National Oceanic and Atmospheric Administration (award NA15OAR4310086). This work was also supported by the Priority Academic Program Development of Jiangsu Higher Education Institutions (PAPD). We acknowledge the World Climate Research Programme's Working Group on Coupled Modelling, which is responsible for CMIP (CMIP5; http://pcmdi9.llnl.gov). SST data sets are downloaded from https://www.esrl.noaa.gov/psd/data/.

References

Adams, J. B., Mann, M. E., & Ammann, C. M. (2003). Proxy evidence for an El Niño-like response to volcanic forcing. *Nature*, *426*(6964), 274–278 . https://doi.org/10.1038/nature02101

Allen, R. J., Evan, A. T., & Booth, B. B. B. (2015). Interhemispheric aerosol radiative forcing and tropical precipitation shifts during the late twentieth century. *Journal of Climate*, *28*(20), 8219–8246. https://doi.org/10.1175/JCLI-D-15-0148.1

Allen, R. J., Norris, J. R., & Kovilakam, M. (2014). Influence of anthropogenic aerosols and the Pacific Decadal Oscillation on tropical belt width. *Nature Geoscience*, *7*(4), 270–274. https://doi.org/10.1038/ngeo2091

Bellucci, A., Mariotti, A., & Gualdi, S. (2017). The role of forcings in the twentieth-century North Atlantic multidecadal variability: The 1940–75 North Atlantic cooling case study. *Journal of Climate*, *30*(18), 7317–7337. https://doi.org/10.1175/JCLI-D-16-0301.1

Boo, K.-O., Booth, B. B. B., Byun, Y.-H., Lee, J., Cho, C., Shim, S., & Kim, K.-T. (2015). Influence of aerosols in multidecadal SST variability simulations over the North Pacific. *Journal of Geophysical Research: Atmospheres*, *120*, 517–531. https://doi.org/10.1002/2014JD021933

Booth, B. B. B., Dunstone, N. J., Halloran, P. R., Andrews, T., & Bellouin, N. (2012). Aerosols implicated as a prime driver of twentieth-century North Atlantic climate variability. *Nature*, *484*(7393), 228–232. https://doi.org/10.1038/nature10946

Boucher, O., Randall, D., Artaxo, P., Bretherton, C., Feingold, G., Forster, P., et al. (2013). Clouds and aerosols. In *Climate Change 2013: The Physical Science Basis. Contribution of Working Group I to the fifth assessment report of the Intergovernmental Panel on Climate Change* (pp. 571–658). Cambridge, UK, and New York: Cambridge University Press.

Cai, W., Borlace, S., Lengaigne, M., van Rensch, P., Collins, M., Vecchi, G., et al. (2014). Increasing frequency of extreme El Niño events due to greenhouse warming. *Nature Climate Change*, *4*(2), 111–116. https://doi.org/10.1038/nclimate2100

Cai, W., Santoso, A., Wang, G., Yeh, S.-W., An, S.-I., Cobb, K. M., et al. (2015). ENSO and greenhouse warming. *Nature Climate Change*, *5*(9), 849–859. https://doi.org/10.1038/nclimate2743

Collins, M., An, S.-I., Cai, W., Ganachaud, A., Guilyardi, E., Jin, F.-F., et al. (2010). The impact of global warming on the tropical Pacific Ocean and El Niño. *Nature Geoscience*, *3*(6), 391–397. https://doi.org/10.1038/ngeo868

Dai, A. (2013). The influence of the inter-decadal Pacific oscillation on US precipitation during 1923–2010. *Climate Dynamics*, *41*(3-4), 633–646. https://doi.org/10.1007/s00382-012-1446-5

Dai, A., & Bloecker, C. E. (2018). Impacts of internal variability on temperature and precipitation trends in large ensemble simulations by two climate models. *Climate Dynamics*. https://doi.org/10.1007/s00382-018-4132-4

Dai, A., Fyfe, J. C., Xie, S.-P., & Dai, X. (2015). Decadal modulation of global surface temperature by internal climate variability. *Nature Climate Change*, *5*(6), 555–559. https://doi.org/10.1038/nclimate2605

Deser, C., Alexander, M. A., Xie, S.-P., & Phillips, A. S. (2010). Sea surface temperature variability: Patterns and mechanisms. *Annual Review of Marine Science*, *2*(1), 115–143. https://doi.org/10.1146/annurev-marine-120408-151453

Dong, B., & Dai, A. (2015). The influence of the Interdecadal Pacific Oscillation on temperature and precipitation over the globe. *Climate Dynamics*, *45*(9-10), 2667–2681. https://doi.org/10.1007/s00382-015-2500-x

Dong, B., Dai, A., Vuille, M., & Elison Timm, O. (2018). Asymmetric modulation of ENSO teleconnections by the Interdecadal Pacific Oscillation. *Journal of Climate*. https://doi.org/10.1175/JCLI-D-17-0663.1

Dong, L., Zhou, T., & Chen, X. (2014). Changes of Pacific decadal variability in the twentieth century driven by internal variability, greenhouse gases, and aerosols. *Geophysical Research Letters*, *41*, 8570–8577. https://doi.org/10.1002/2014GL062269

England, M. H., McGregor, S., Spence, P., Meehl, G. A., Timmermann, A., Cai, W., et al. (2014). Recent intensification of wind-driven circulation in the Pacific and the ongoing warming hiatus. *Nature Climate Change*, *4*(3), 222–227. https://doi.org/10.1038/nclimate2106

Fyfe, J. C., & Gillett, N. P. (2014). Recent observed and simulated warming. *Nature Climate Change*, *4*(3), 150–151. https://doi.org/10.1038/nclimate2111

Fyfe, J. C., Gillett, N. P., & Zwiers, F. W. (2013). Overestimated global warming over the past 20 years. *Nature Climate Change*, *3*(9), 767–769. https://doi.org/10.1038/nclimate1972

Fyfe, J. C., Meehl, G. A., England, M. H., Mann, M. E., Santer, B. D., Flato, G. M., et al. (2016). Making sense of the early-2000s warming slowdown. *Nature Climate Change*, *6*(3), 224–228. https://doi.org/10.1038/nclimate2938

Gu, G., & Adler, R. F. (2015). Spatial patterns of global precipitation change and variability during 1901–2010. *Journal of Climate*, *28*(11), 4431–4453. https://doi.org/10.1175/JCLI-D-14-00201.1

Henley, B. J., Gergis, J., Karoly, D. J., Power, S., Kennedy, J., & Folland, C. K. (2015). A tripole index for the Interdecadal Pacific Oscillation. *Climate Dynamics*, *45*(11-12), 3077–3090. https://doi.org/10.1007/s00382-015-2525-1

Hirahara, S., Ishii, M., & Fukuda, Y. (2014). Centennial-scale sea surface temperature analysis and its uncertainty. *Journal of Climate*, *27*(1), 57–75. https://doi.org/10.1175/JCLI-D-12-00837.1

Huang, B., Thorne, P. W., Banzon, V. F., Boyer, T., Chepurin, G., Lawrimore, J. H., et al. (2017). Extended Reconstructed Sea Surface Temperature version 5 (ERSSTv5), upgrades, validations, and intercomparisons. *Journal of Climate*, *30*(20), 8179–8205. https://doi.org/10.1175/JCLI-D-16-0836.1

Kaplan, A., Cane, M. A., Kushnir, Y., Clement, A. C., Blumenthal, M. B., & Rajagopalan, B. (1998). Analyses of global sea surface temperature 1856-1991. *Journal of Geophysical Research*, *103*, 18,567–18,589. https://doi.org/10.1029/97JC01736

Khodri, M., Izumo, T., Vialard, J., Janicot, S., Cassou, C., Lengaigne, M., et al. (2017). Tropical explosive volcanic eruptions can trigger El Niño by cooling tropical Africa. *Nature Communications*, *8*(1), 778. https://doi.org/10.1038/s41467-017-00755-6

Kosaka, Y., & Xie, S.-P. (2013). Recent global-warming hiatus tied to equatorial Pacific surface cooling. *Nature*, *501*(7467), 403–407. https://doi.org/10.1038/nature12534

Li, J., Xie, S.-P., Cook, E. R., Morales, M. S., Christie, D. A., Johnson, N. C., et al. (2013). El Niño modulations over the past seven centuries. *Nature Climate Change*, *3*(9), 822–826. https://doi.org/10.1038/nclimate1936

Luo, J., Sasaki, W., & Masumoto, Y. (2012). Indian Ocean warming modulates Pacific climate change. *Proceedings of the National Academy of Sciences of the United States of America*, *109*(46), 18,701–18,706. https://doi.org/10.1073/pnas.1210239109

Luo, J., Wang, G., & Dommenget, D. (2018). May common model biases reduce CMIP5's ability to simulate the recent Pacific La Niña-like cooling? *Climate Dynamics*, *50*(3-4), 1335–1351. https://doi.org/10.1007/s00382-017-3688-8

Maher, N., McGregor, S., England, M. H., & Sen Gupta, A. (2015). Effects of volcanism on tropical variability. *Geophysical Research Letters*, *42*, 6024–6033. https://doi.org/10.1002/2015GL064751

Mann, M. E., Cane, M. A., Zebiak, S. E., & Clement, A. (2005). Volcanic and solar forcing of the tropical Pacific over the past 1000 years. *Journal of Climate*, *18*(3), 447–456. https://doi.org/10.1175/JCLI-3276.1

Mantua, N. J., Hare, S. R., Zhang, Y., Wallace, J. M., & Francis, R. C. (1997). A Pacific interdecadal climate oscillation with impacts on salmon production. *Bulletin of the American Meteorological Society*, *78*, 1069–1079. https://doi.org/10.1175/1520-0477(1997)078<1069:APICOW>2.0.CO;2

McGregor, S., Timmermann, A., Stuecker, M. F., England, M. H., Merrifield, M., Jin, F.-F., & Chikamoto, Y. (2014). Recent Walker circulation strengthening and Pacific cooling amplified by Atlantic warming. *Nature Climate Change*, *4*(10), 888–892. https://doi.org/10.1038/nclimate2330

Meehl, G. A., Hu, A., Arblaster, J. M., Fasullo, J., & Trenberth, K. E. (2013). Externally forced and internally generated decadal climate variability associated with the Interdecadal Pacific Oscillation. *Journal of Climate*, *26*(18), 7298–7310. https://doi.org/10.1175/JCLI-D-12-00548.1

Meehl, G. A., Hu, A., & Santer, B. D. (2009). The mid-1970s climate shift in the Pacific and the relative roles of forced versus inherent decadal variability. *Journal of Climate*, *22*(3), 780–792. https://doi.org/10.1175/2008JCLI2552.1

Morice, C. P., Kennedy, J. J., Rayner, N. A., & Jones, P. D. (2012). Quantifying uncertainties in global and regional temperature change using an ensemble of observational estimates: The HadCRUT4 data set. *Journal of Geophysical Research*, *117*, D08101. https://doi.org/10.1029/2011JD017187

Myhre, G., Shindell, D., Bréon, F.-M., Shindell, D., Bréon, F.-M., Collins, W., et al. (2013). Anthropogenic and Natural Radiative Forcing. In *Climate change 2013: The physical science basis. Contribution of Working Group I to the fifth assessment report of the Intergovernmental Panel on*

Climate Change (pp. 659–740). Cambridge, UK, and New York: Cambridge University Press. https://doi.org/10.1017/CBO978 1107415324.018

Power, S., Casey, T., Folland, C., Colman, A., & Mehta, V. (1999). Interdecadal modulation of the impact of ENSO on Australia. *Climate Dynamics*, *15*(5), 319–324. https://doi.org/10.1007/s003820050284

Santer, B. D., Bonfils, C., Painter, J. F., Zelinka, M. D., Mears, C., Solomon, S., et al. (2014). Volcanic contribution to decadal changes in tropospheric temperature. *Nature Geoscience*, *7*(3), 185–189. https://doi.org/10.1038/ngeo2098

Si, D., & Hu, A. (2017). Internally generated and externally forced multidecadal oceanic modes and their influence on the summer rainfall over East Asia. *Journal of Climate*, *30*(20), 8299–8316. https://doi.org/10.1175/JCLI-D-17-0065.1

Smith, D. M., Booth, B. B. B., Dunstone, N. J., Eade, R., Hermanson, L., Jones, G. S., et al. (2016). Role of volcanic and anthropogenic aerosols in the recent global surface warming slowdown. *Nature Climate Change*, *6*(10), 936–940. https://doi.org/10.1038/nclimate3058

Steinman, B. A., Mann, M. E., & Miller, S. K. (2015). Atlantic and Pacific multidecadal oscillations and Northern Hemisphere temperatures. *Science*, *347*(6225), 988–991. https://doi.org/10.1126/science.1257856

Takahashi, C., & Watanabe, M. (2016). Pacific trade winds accelerated by aerosol forcing over the past two decades. *Nature Climate Change*, *6*(8), 768–772. https://doi.org/10.1038/nclimate2996

Taylor, K. E., Stouffer, R. J., & Meehl, G. A. (2012). An overview of CMIP5 and the experiment design. *Bulletin of the American Meteorological Society*, *93*(4), 485–498. https://doi.org/10.1175/BAMS-D-11-00094.1

Williams, K. D., Jones, A., Roberts, D. L., Senior, C. A., & Woodage, M. J. (2001). The response of the climate system to the indirect effects of anthropogenic sulfate aerosol. *Climate Dynamics*, *17*(11), 845–856. https://doi.org/10.1007/s003820100150

Xu, Y., & Hu, A. (2018). How would the 21st-century warming influence Pacific decadal variability and its connection to North American rainfall: Assessment based on a revised procedure for IPO/PDO. *Journal of Climate*, *31*(4), 1547–1563. https://doi.org/10.1175/JCLI-D-17-0319.1

Zhang, R., Delworth, T. L., Sutton, R., Hodson, D. L. R., Dixon, K. W., Held, I. M., et al. (2013). Have aerosols caused the observed Atlantic multidecadal variability? *Journal of the Atmospheric Sciences*, *70*(4), 1135–1144. https://doi.org/10.1175/JAS-D-12-0331.1

Zhang, Y., Wallace, J. M., & Battisti, D. S. (1997). ENSO-like interdecadal variability: 1900–93. *Journal of Climate*, *10*(5), 1004–1020. https://doi.org/10.1175/1520-0442(1997)010<1004:ELIV>2.0.CO;2